Numerical modelling of complex modulus tests in direct tension-compression on asphalt concrete using the 2D Discrete Element Method

Léo Coulon, Georg Koval, Cyrille Chazallon, Jean-Noël Roux

Numerical modelling of complex modulus tests in direct tension-compression on asphalt concrete using the 2D Discrete Element Method

Léo COULON[1*], Georg KOVAL[1], Cyrille CHAZALLON[1] and Jean-Noël ROUX[2]

*corresponding author: leo.coulon@insa-strasbourg.fr
[1]Laboratoire ICube (CNRS, UMR 7357), INSA Strasbourg, France
[2] Laboratoire Navier (CNRS, UMR 8205), Université Gustave Eiffel, France

Abstract. The VENoL analytical model was developed to reproduce the nonlinear viscoelastic behaviour of asphalt concrete in dynamic analysis. In this paper, it is integrated as a contact law in a 2D model using the Discrete Element Method. The commercial software PFC version 5 from Itasca is used to apply the method. The asphalt is modelled on a macroscopic scale. The VENoL model is applied in the numerical code without any recalibration of its analytical parameters. Particular care is taken to model the Poisson's ratio, whose value depends on the test conditions. This integration is checked by comparing, for complex modulus tests in direct tension-compression, the results obtained for the numerical model with those extracted from the literature. The results show that with a single set of parameters, it is possible to model the effects of frequency and temperature. Despite the use of a macroscopic scale, the model is also able to model porosity effects through the mechanisms of DEM.

Keywords: Complex modulus test, Discrete Element Method, VENoL model.

1 Introduction

In France, the viscoelastic nature of asphalt concrete is assessed in laboratory with complex modulus tests complying with standard NF EN 12697-26 (June 2018) [1]. The VENoL analytical model was developed on the basis of these tests with the aim of reproducing the nonlinear viscoelastic behaviour of asphalt mixes in dynamic analysis [2]. The work presented in this paper is devoted to the implementation of this model as a contact law in a discrete numerical approach.

Discrete methods consist of a combination of distinct elements, interacting with each other according to behaviour laws. If at each time step, the contact forces acting on each element are known, the motion equation of each element is deduced from the Newton's second law of motion. Discrete methods are usually used for discontinuous media (heterogeneous materials, presence of multiple cracks). However, they require long computation times, because of the use of small time steps to maintain model stability. In the field of bituminous materials, discrete methods have already been employed by several

authors [3-5]. The Burgers model is regularly used as a contact law, and a constant Poisson's ratio is often considered.

In this article, in addition to using the VENoL model as a contact law, a second innovation is introduced by considering variations in the Poisson's ratio according to test conditions. The discrete approach adopted is the Discrete Element Method (DEM) of CUNDALL and STRACK [6]. The commercial software PFC version 5 from Itasca is used. The modelling is performed on a macroscopic scale, which means that the numerical particles represent asphalt aggregates (binder + aggregate). Although the asphalt concrete is modelled here continuously, DEM was preferred to the finite element method for several reasons. Firstly, DEM makes it easy to introduce relatively complex behaviour laws at the contact level. Secondly, the model is developed with a view to evolving towards smaller scales and adding progressive multi-cracking of the medium. Modelling is carried out in two dimensions to reduce computation time.

The article is built in three sections. First, a resume of the VENoL model is provided. Then, the numerical process for making complex modulus tests is detailed. Finally, the numerical model is applied to a bituminous mixture from FREIRE's thesis [7]. The experimental data come from direct tension-compression tests on a cylindrical specimen (DTC-CY). This homogeneous test provides access to measurements of the complex Poisson's ratio, a necessary parameter in the calibration of the numerical model.

2 VENoL model description

The VENoL model is based on a Kelvin-Voigt differential equation that results directly from the complex stiffness modulus E^* relation obtained by dividing the stress signal $\sigma^*(t)$ by the strain signal $\varepsilon^*(t)$.

$$\sigma^*(t) = E^* \cdot \varepsilon^*(t) \tag{1}$$

Indeed, the equation can be reduced by dividing the imaginary part $\mathrm{Im}(E^*)$ by the signal pulsation ω. A term $i\omega$ then appears as a factor.

$$\sigma^*(t) = \left[\mathrm{Re}(E^*) + i\omega \cdot \frac{\mathrm{Im}(E^*)}{\omega}\right] \cdot \varepsilon^*(t) \tag{2}$$

The multiplication of $i\omega$ by $\varepsilon^*(t)$ gives the derived function, the strain rate $\dot{\varepsilon}^*(t)$. The real part $\mathrm{Re}(E^*)$ is then replaced by the symbol $\Re_E$, named the stiffness component, while the term $\mathrm{Im}(E^*)/\omega$ is replaced by the symbol $\Im_\eta$, the viscosity component.

$$\sigma^*(t) = \Re_E \cdot \varepsilon^*(t) + \Im_\eta \cdot \dot{\varepsilon}^*(t) \tag{3}$$

The VENoL model operates on the principle of variable parameters, which means that the two components $\Re_E$ and $\Im_\eta$ fluctuate by means of analytical equations to take account of the influence of loading conditions on viscoelasticity. $\Re_E$ and $\Im_\eta$ are thus defined as a function of the pulsation ω using Carreau-Yasuda-type equations (CY) [2].

The influence of other conditions is added by means of superposition principles. The effect of temperature T is provided by the Time-Temperature Superposition Principle (TTSP), whose translation factor a_T is defined using the Williams-Landel-Ferry law

(WLF). The effect of strain amplitude ε_0 (non-linearity) is given by the Time-Amplitude Semi-Superposition Principle (TASSP), whose translation factors a_A and b_A are calibrated using WLF-type equations [2]. These two principles can be combined to form the Time-Temperature-Amplitude Semi-Superposition Principle (TTASSP). The reduced pulsation ω_{R-TA} and the reduced viscosity component $\Im_{\eta,R-TA}$ are then calculated as follows:

$$a_{TA} = a_T \cdot a_A \tag{4}$$

$$\omega_{R-TA} = a_{TA} \cdot \omega \tag{5}$$

$$\Im_{\eta,R-TA} = \frac{\Im_\eta}{a_{TA} \cdot b_A} \tag{6}$$

The VENoL model can also be used to reproduce the real part of the complex Poisson's ratio ν^*, observing that it varies analogously to the phase angle φ_{E^*} as a function of the reduced pulsation. A simple scaling factor k_{ν^*} is then required, combined with a lower limit ν_{inf}.

$$\mathrm{Re}(\nu^*) \approx \nu_{inf} + k_{\nu^*} \cdot \varphi_{E^*} \tag{7}$$

The imaginary part of the complex Poisson's ratio is assumed to be null, as it is very small compared with the real part. A biasing effect might be at the origin of the imaginary part. Thus, $\nu \approx \mathrm{Re}(\nu^*)$.

3 Numerical process

3.1 Design of the numerical specimen

The walls of a mould with the dimensions of the test piece are first created. A provisional contact law "Linear Model" is then imposed for each contact newly created between two particles. This law is a Kelvin-Voigt model programmed in PFC which does not admit tensile behaviour, which means that the contact disappears when the gap g between the edges of the two particles becomes greater than the reference gap g_r. This reference gap g_r is set to zero, so contact is only active when the particles overlap. A fictitious stiffness and a fictitious viscous damping are assigned to the model. Particles are then generated and automatically distributed within the mould according to characteristics provided by the user: a targeted porosity, a uniform distribution of particle radii bounded by a minimum and a maximum radius, a controlled random generation number between 10,001 and 19,999 to which a fixed particle configuration corresponds, and a density. In this article, targeted porosity is defined as the ratio of the total area of generated particles to the area of the mould, disregarding overlaps.

When two particles overlap ($g < 0$), a reaction force is created, pushing the particles apart. Calculation cycles are then run until the system stabilises thanks to the damping effect of the Kelvin-Voigt model. The residual forces are then reset to zero and the

mould walls are removed. Afterwards, the law of active contact ($g < g_r$) is replaced by that defined in section 3.2, which maintains active contact in tension ($g > g_r$). The gap g between each connected particle is then defined as the new reference gap g_r, so that forces are maintained at zero when the test starts. And any creation of new contact during the test is deactivated by imposing the contact law "Null Model" on non-active contacts (potential contact between two neighbouring particles that becomes active when $g < g_r$), which maintains zero force and zero moment.

3.2 Contact law

The provisional contact law "Linear Model" used to design the specimen in section 3.1 is replaced by the contact law "Linear Contact Bond Model", which also corresponds to a Kelvin-Voigt model consisting of a spring of stiffness k and a viscous dashpot of damping constant c connected in parallel. This model maintains active contact in compression ($g < g_r$) and tension ($g > g_r$).

Figure 1 illustrates a newly-created contact between two particles i and j with different radii R_i and R_j and masses m_i and m_j. In the initial state, when $g = g_r$, the work on the contact is null and the centers of the two particles are exactly separated by a distance $l_{0,ij}$. The contact is represented by a 2D cylinder of length l_{ij} and radius r equal to the minimum of the radii of the two particles it connects. In the local plane of the contact, each of the particles is free to move along a normal direction $\vec{n}_{ij}$ and a shear direction $\vec{s}_{ij}$, as well as to rotate around its center. The differential displacement and rotation velocities between the two particles generate length variations δ_n and δ_s and velocity variations $\dot{\delta}_n$ and $\dot{\delta}_s$ at the contact. Normal and tangential forces F_n and F_s are consequently generated by the Kelvin-Voigt models.

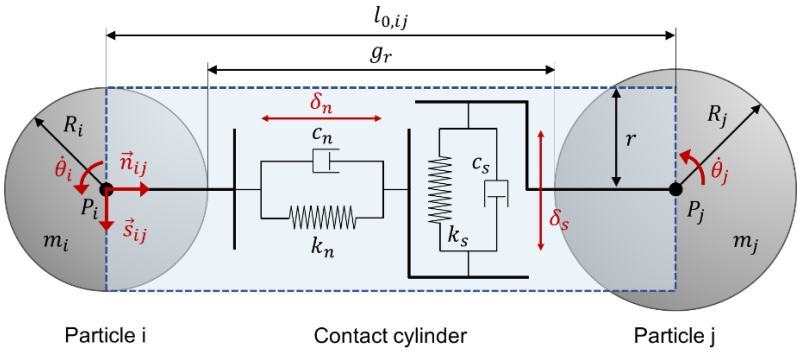

Fig. 1. DEM representation of a viscoelastic contact between two particles in the initial state.

The PFC software operates with real numbers only. Considering the 2D geometry of the contact cylinder, the real part of the complex differential equation of the VENoL model can be written in terms of force and displacement. As the VENoL model was developed from the axial measurements of the DTC-CY test, its equation must be assimilated to the normal direction of the contact (Eqs. 8 to 11). In the shear direction, k_s

and c_s are respectively defined as a function of k_n and c_n using a coefficient λ_s which symbolises the shear/normal ratio (Eqs. 12 to 15). In DEM, the value of the Poisson's ratio depends only on λ_s. Depending on the values taken by λ_s, the level of the complex stiffness modulus of the numerical specimen may be affected. This needs to be corrected by a coefficient λ_n. α_1, α_2 and α_3 are adjustment coefficients for λ_n and λ_s. α_{acc} is a calculation acceleration factor. It should be used sparingly, as choosing it too small can lead to inertial effects.

Normal contact "n"		**Shear contact "s"**	
$F_n(t) = k_n \cdot \delta_n(t) + c_\eta \cdot \dot{\delta}_n(t)$	(8)	$F_s(t) = k_s \cdot \delta_s(t) + c_s \cdot \dot{\delta}_s(t)$	(12)
$k_n = \alpha_{acc} \cdot \lambda_n \cdot \frac{2r}{l_{0,ij}} \Re_E(\omega_{R-TA})$	(9)	$k_s = \lambda_s \cdot k_n$	(13)
$c_n = \alpha_{acc} \cdot \lambda_n \cdot \frac{2r}{l_{0,ij}} \Im_\eta(\omega_{R-TA})$	(10)	$c_s = \lambda_s \cdot c_n$	(14)
$\lambda_n = \frac{1}{\alpha_1 \cdot [1-\alpha_2 \cdot \nu(\omega_{R-TA})]}$	(11)	$\lambda_s = \frac{1-\alpha_3 \cdot \nu(\omega_{R-TA})}{1+\nu(\omega_{R-TA})}$	(15)

3.3 Test equipment

The loading plates are made up of groups of particles whose movements are constrained. For the DTC-CY test, the upper loading plate is used to apply vertical displacements (Fig. 2). The y displacements of its particles are therefore kept free, but the x displacements and rotations θ are blocked (embedding). The lower loading plate is held immobile by the complete blocking of its particles (embedding). The plates are also used to measure the reaction forces exerted by the specimen on them, in order to calculate the evolution of axial stress during the test. And some particles are targeted to be used as axial and radial displacement sensors to determine strain. Each sensor is doubled to calculate an average over two measurements.

3.4 Complex modulus test process

The user provides the numerical program with the test conditions: frequency, loading strain amplitude and surrounding temperature. The test is performed by applying a sinusoidal vertical displacement to the upper loading plate. The displacement amplitude is gradually increased on the first cycle from zero up to the value set by the user. Two to three loading cycles are sufficient to obtain material properties, as test stabilization generally occurs between one and two cycles.

The calculation time step is fixed during the test. A second time discretisation is introduced to record the complex stiffness modulus and complex Poisson's ratio measurements. At the time step following the measurements, the contact properties k_n, c_n and k_s, c_s are updated according to PSETA, in other words, according to the contact strain amplitude (non-linearity).

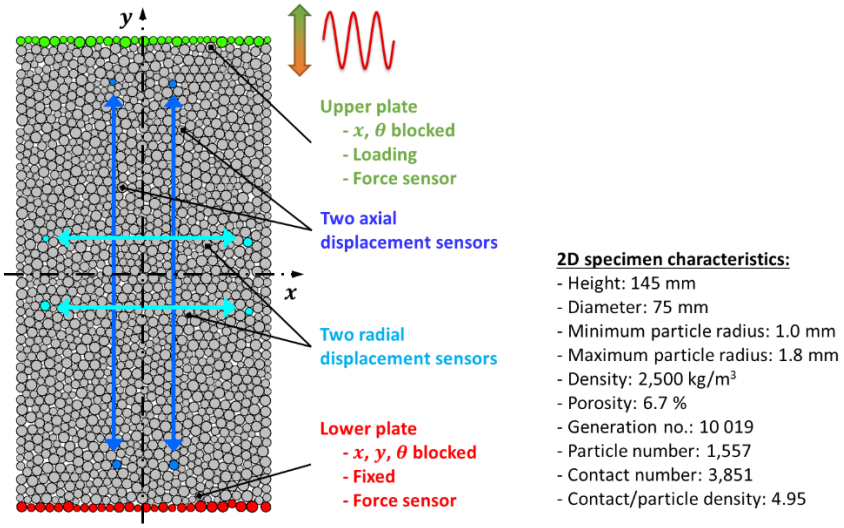

Fig. 2. Example of equipment on the numerical test piece PFC-F-C-10019.

4 Application example

This example is based on experimental results obtained by FREIRE from DTC-CY complex modulus tests carried out at 50 µm/m on specimen A1-H3 [7] (Fig. 3, "CM-Exp A1-H3"). The cylindrical specimen has a height of 140 mm, a diameter of 75 mm and an estimated porosity of 6.2%. This specimen is characterized by a BBSG 0/10 mm (a French asphalt concrete meaning *Béton Bitumineux Semi-Grenu*) containing 20% RAP (Reclaimed Asphalt Pavement) and a pure bitumen of penetration grade 35/50 dosed at 4.40%. The true density obtained for this mixture is 2510 kg/m^3.

The VENoL analytical model is first fitted to the experimental data (Fig. 3, "CM-Mod"). The parameter values are then integrated into the DEM code. Then, the parameters α_1, α_2 and α_3 are calibrated using a numerical specimen of similar porosity to the A1-H3 reference specimen (Fig. 3, "CM-DEM PFC-F-C-10019"). Complex modulus tests are then carried out on five other numerical specimens, two with similar porosities (10005 and 10014) and three with different porosities (10003, 10044 and 10023).

For close porosities, slight fluctuations in modulus are observed due to different particle distributions and arrangements (Fig. 3a). This effect tends to disappear with smaller particles. An increase in porosity leads to a decrease in the density of contacts per particle, and hence to an decrease in the complex stiffness modulus. This direction is in line with the literature, but it will be necessary to verify later that the modulus differentials obtained for various porosities corroborate those obtained experimentally. Porosity has a proportional influence on the real and imaginary parts. This means that an increase in porosity leads to a decrease in the modulus norm, but does not affect the phase angle. Moreover, for a constant Poisson's ratio, the ratio between the moduli of two different porosities remains constant regardless of temperature and frequency.

At the level of the real part of the complex Poisson's ratio, it is more difficult to determine a porosity trend, as it is obscured by its sensitivity to particle distribution and arrangement (Fig. 3b). It was also hoped for a while that the DEM mechanisms associated with nonlinearity effects would automatically model the imaginary part of the complex Poisson's ratio by simply implementing the real part. However, the real part remains systematically null. It could therefore well be linked to material properties and not to a biasing effect as has been assumed. Further investigations are required.

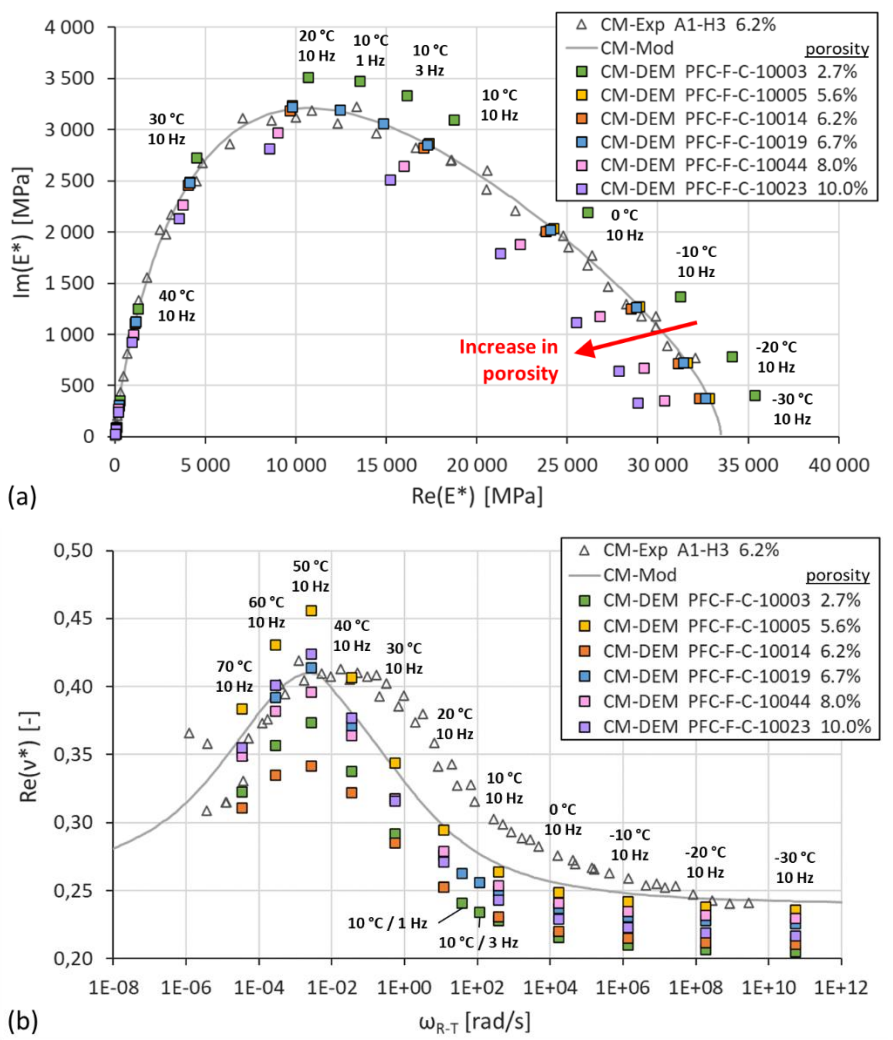

Fig. 3. FREIRE's asphalt concrete – Specimen A1-H3 – DTC-CY, CM, 50 µm/m. Effect of numerical porosity in DEM on the complex stiffness modulus in the Cole-Cole plane (a) and on the real part Re(ν^*) of the complex Poisson's ratio (b). Superposition of experimental data "Exp", analytical model VENoL "Mod" and DEM simulations.

5 Conclusion

The VENoL analytical model was developed to reproduce the nonlinear viscoelastic behaviour of asphalt concrete in dynamic analysis. This article presents the approach used to implement it as a contact law within a DEM-based numerical code. This approach is validated by the numerical model's ability to reproduce DTC-CY complex modulus tests of an asphalt concrete extracted from the literature, at different temperatures and frequencies, for a single set of parameters. Thanks to the laws of the analytical model, the numerical model can also reproduce variations in the real part of the complex Poisson's ratio. Although the model is designed on a macroscopic scale, it is also able to model the mesoscopic effect of porosity using DEM mechanisms.

Acknowledgements

The authors warmly thank the author Reuber A. FREIRE, and his thesis directors Hervé DI BENEDETTO and Cédric SAUZÉAT, for kindly providing some experimental data presented in his thesis [7].

Disclosure statement No potential conflict of interest was reported by the authors.

Funding

The work presented in this paper was supported by the French institution *Agence Nationale de la Recherche* (ANR-MOVEDVDC project, ref. ANR-17-CE22-0014-03, and ANR BINARY project, ref. ANR-19-CE22-0001).

References

1. AFNOR (2018, June). *Mélanges bitumineux – Méthodes d'essai – Partie 26 : Module de rigidité* (NF EN 12697-26, 54 p). [In French].
2. COULON, L., KOVAL, G., CHAZALLON, C. et ROUX, J.-N. (2021). Analytical modelling of complex stiffness modulus tests in direct tension-compression on asphalt concrete and nonlinearity effect due to strain amplitude. *Road Materials and Pavement Design*, vol. 24, no. 1, p. 216-246. https://doi.org/10.1080/14680629.2021.2014349
3. YU, H., & SHEN, S. (2013). A micromechanical based three-dimensional DEM approach to characterize the complex modulus of asphalt mixtures. *Construction and Building Materials*, vol. 38, p. 1089-1096. https://doi.org/10.1016/j.conbuildmat.2012.09.036
4. DONDI, G., VIGNALI, V., PETTINARI, M., MAZZOTTA, F., SIMONE, A., & SANGIORGI, C. (2014). Modeling the DSR complex shear modulus of asphalt binder using 3D discrete element approach. *Construction and Building Materials*, vol. 54, p. 236-246. https://doi.org/10.1016/j.conbuildmat.2013.12.005
5. QUEZADA, J. C., & CHAZALLON, C. (2020). Complex modulus modeling of asphalt concrete mixes using the Non-Smooth Contact Dynamics method. *Computer and Geotechnics*, vol. 117, 9 p. https://doi.org/10.1016/j.compgeo.2019.103255
6. CUNDALL, P. A., & STRACK, O. D. L. (1979). A discrete numerical model for granular assemblies. *Géotechnique*, vol. 29, no. 1, p. 47–65. https://doi.org/10.1680/geot.1979.29.1.47
7. FREIRE, R. A. (2020). *Use of fiberglass geogrids to the reinforcement of bituminous mixtures layers* (293 p.) [PhD thesis]. ENTPE, Université de Lyon, France. HAL theses. https://theses.hal.science/tel-03249370